Entropic Commensurate-Incommensurate Transition

Nikolai Nikola, Daniel Hexner, and Dov Levine
Department of Physics, Technion-IIT, 32000 Haifa, Israel
(Received 3 December 2012; published 19 March 2013)

The equilibrium properties of a minimal tiling model are investigated. The model has extensive ground state entropy, with each ground state having a quasiperiodic sequence of rows. It is found that the transition from the ground state to the high temperature disordered phase proceeds through a sequence of periodic arrangements of rows, in analogy with the commensurate-incommensurate transition. We show that the effective free energy of the model resembles the Frenkel-Kontorova Hamiltonian, but with temperature playing the role of the strength of the substrate potential, and with the competing lengths not explicitly present in the basic interactions.

DOI: 10.1103/PhysRevLett.110.125701 PACS numbers: 64.60.De, 61.44.Br, 61.44.Fw

Tilings provide a simple means to model systems with both simple and complex ground states. As statistical mechanical models, they include such systems as the Ising and Potts models, as well as other models with discrete spin variables [1]. The class of tilings, however, is much larger [2], and includes the various nonperiodic Wang tilings [3], the quasiperiodic Penrose tilings, the asymptotically isotropic Pinwheel tiling [4], and the recently discovered generalizations of the Rudin-Shapiro sequence, which are neither periodic nor quasiperiodic [5].

The statistical mechanical behavior of tiling models is rich, and, as yet, largely uncharted. Apart from results which may be transcribed from discrete spin models, only a very small number of systems have been studied. First, a model based on the Amman set of 16 Wang tiles with quasiperiodic ground states was studied by several authors [6–8]. It appears that this model undergoes a continuous phase transition from a disordered state to a quasiperiodic phase, and its nonequilibrium behavior was studied in the context of spin glasses. A variation of the model allowing more complicated interactions and vacancies shows a first order transition [9]. Hierarchical tilings [10] have also been studied, and a very recent model [11] possesses limit-periodic ground states which undergo a series of phase transitions where motifs of ever larger scales order as the temperature is lowered. Finally, we note some recent studies [12,13] on models with a large number of degenerate disordered ground states aimed at studying glasses.

In this Letter, we study the equilibrium behavior of a model based on the 13-tile Kari-Culik (KC) set [14,15] of Wang tiles, both numerically and analytically. The KC set is the smallest known *aperiodic* set—it is the smallest set of tiles which can tile the plane, but not periodically. Allowed juxtapositions of tiles are enforced by matching rules, and these in turn induce a Hamiltonian: every matching rule violation is penalized by a positive energy, while allowed matchings have zero energy. In what follows, we shall denote the energy cost of mismatching adjacent vertical or horizontal edges by J_x or J_y, respectively.

We shall argue that the equilibrium behavior of this system is analogous to the Frenkel-Kontorova (FK) model [16] of the commensurate-incommensurate (CI) transition. The FK model describes a chain of masses which are connected by springs and subjected to a periodic substrate potential. It exhibits rich behavior due to competition between these two interactions, each of which favors ordering with a different wavelength. However, in marked contrast with the FK model, where the favored length scales are present in the Hamiltonian, in the KC model they emerge spontaneously, from only nearest-neighbor interactions. Moreover, the role of substrate potential strength in the FK model is played by the temperature in the KC model. In this sense, the KC system exhibits an *entropic* CI transition.

As indicated in Fig. 1, the 13 KC tiles may be divided into two groups, which we will call types A and B. The markings on the edges of the tiles indicate the matching rules—abutting edges of adjacent tiles have the same markings in a perfect tiling. It is readily seen that in an undefected tiling, a given row can consist of A or B type tiles only, with no mixing, and thus, we may characterize a row as being A type or B type.

The KC tiling differs from other tilings studied in that it is not generated by recursive substitution (inflation) [2,17], and by the fact that it has a ground state degeneracy with

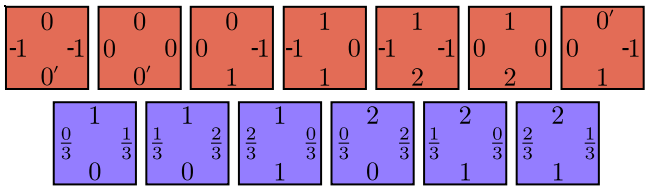

FIG. 1 (color online). The 13 KC tiles. The seven upper tiles are type A, and the six lower tiles are type B. Note that $\frac{0}{3}$, 0, and $0'$ are considered different markings.

 © 2013 American Physical Society

extensive entropy. This should be contrasted with tilings created from a simple inflation rule where the degeneracy scales as a power of the system size [6]. All the ground states, however, are characterized by a quasiperiodic arrangement of A-type and B-type rows. The finite temperature behavior of this model is striking—as the temperature is increased from zero, the rows, still identifiable as A or B type, order periodically with a decreasing period. At high enough temperatures, the rows lose their A or B identity, and the system becomes disordered.

The proof that there exists a zero-energy ground state is equivalent to showing that a perfect tiling exists. To do this [18], we note that there are two numbers which characterize the nth row in a perfect tiling—the "frequency" α_n and the number q_n which are related through the mapping

$$\alpha_{n+1} = q_n \alpha_n, \tag{1}$$

where

$$q_n = \begin{cases} 2 & \frac{1}{3} \le \alpha_n < 1 \\ \frac{1}{3} & 1 \le \alpha_n < 2. \end{cases} \tag{2}$$

Note that we shall take n to increase in the negative y direction.

The reason for dividing the tile set into the A and B groups becomes apparent if we denote the markings of the top, bottom, right, and left edges of a tile by $\{t, b, r, l\}$, as shown in Fig. 2. When needed, we shall indicate the position of the tile as a subscript; thus $t_{m,n}$ refers to the marking of the top edge of the tile centered at (m, n), etc. It is easily verified by inspecting Fig. 1 that the markings on each tile satisfy the relation

$$q_n t_{m,n} + l_{m,n} = r_{m,n} + b_{m,n}, \tag{3}$$

with a tile of type A or B having $q_n = 2$ or $\frac{1}{3}$, respectively. The mapping $\alpha_{n+1} = q_n \alpha_n$ has no periodic points, since $\alpha_{n+q}/\alpha_n = 2^p/3^{q-p} \neq 1$ for any positive integers p and q; this implies that the resultant tilings are not periodic.

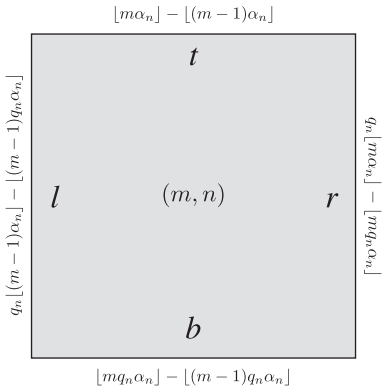

FIG. 2. The marking scheme for the tile at (m, n). Note that n increases in the negative y direction.

The α_n are distributed densely, but not uniformly, in the range $(\frac{1}{3}, 2)$.

To show that a perfect tiling exists, we must solve Eq. (3) for all m, n with q_n derived from Eqs. (1) and (2) while demanding that $b_{m,n} = t_{m,n+1}$ and $l_{m,n} = r_{m-1,n}$. It is easily verified that the markings

$$\begin{aligned} t_{m,n} &= \lfloor m\alpha_n \rfloor - \lfloor (m-1)\alpha_n \rfloor, \\ r_{m,n} &= q_n \lfloor m\alpha_n \rfloor - \lfloor mq_n\alpha_n \rfloor, \end{aligned} \tag{4}$$

constitutes a solution, where $\lfloor x \rfloor$ is the greatest integer less than or equal to x (see Fig. 2); this is one example of a perfect tiling.

To facilitate later discussion, we shall employ a useful mapping. Let us define the variable $\phi_n = n\omega_0$, where $\omega_0 = \log 2/\log(6) \approx 0.3868$. Decomposing ϕ_n into its integer and fractional parts gives

$$\phi_n = \lfloor n\omega_0 \rfloor + \{\phi_n\}, \tag{5}$$

where $\{\phi_n\}$, the fractional part of ϕ_n, is defined through its relation to α_n by

$$\{\phi_n\} = \frac{\log(\alpha_n) + \log(3)}{\log(2) + \log(3)}. \tag{6}$$

This maps $\alpha_n \in [\frac{1}{3}, 2)$ onto $\{\phi_n\} \in [0, 1)$, and allows us to obtain [19] an explicit formula for q_n :

$$q_n = \left(\frac{1}{3} - 2\right)[\lfloor (n+1)\omega_0 \rfloor - \lfloor n\omega_0 \rfloor] + 2.$$

Sequences of this type are called *Sturmian sequences*, and are well known in the context of automatic sequences [20]. Here ω_0 is irrational, and this gives a quasiperiodic sequence of the two "letters" 2 and $\frac{1}{3}$, with the consequence that, in the ground state, the rows appear in a quasiperiodic sequence.

As noted above, this ground state is only one of many, and in fact, there is an extensive ground state entropy [19]. This may be inferred from Fig. 3, where two patches with the same markings on their exterior are presented (there exist larger patches with the same property as well). This means that starting from some given ground state, we may obtain another by randomly exchanging the patches shown in Fig. 3 (and any other pair of patches with the same exterior markings), provided, as we have verified [19], that

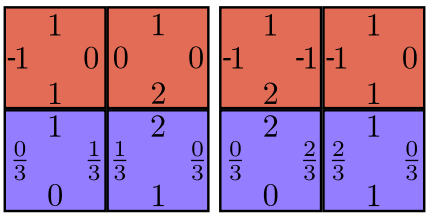

FIG. 3 (color online). An example of two different 2×2 patches with the same outer markings; these may be exchanged with no matching rule violations.

they appear with a finite density in the ground state. This implies that almost all of the ground states are disordered in the sense that their patch entropy [21] scales as the patch size for large enough patches. This notwithstanding, in all the ground states, the rows are arranged in a quasiperiodic sequence of A type and B type, and it is also true that α_n is unchanged for each row [19], which is relevant to what follows.

Numerical studies of this model show that as the temperature is raised from 0, it goes through a series of phase transitions, where the A-B sequence of rows is periodic, and where the period decreases with increasing temperature. In analogy to the CI transition, we shall refer to these periodic phases as *commensurate phases*. In Fig. 4, we show a portion of a time averaged configuration from a 150×150 system (with $J_x = J_y$) at $T = 0.304$ (in units of J_x), which was obtained by parallel tempering, where the color coding is as in Fig. 1. The A-B sequence is periodic with period 8, with 3 B rows per period. Characteristic defects are also present. At high enough temperature, of course, the rows lose their A or B character, and the system goes to a disordered phase.

The different phase transitions are best traced by the winding number $\Omega = \frac{N_B}{N_A+N_B}$. Since at low T the rows are essentially pure type A or B, Ω essentially counts the fraction of type B rows in the system. For an ensemble of systems at any given temperature, Ω may take a variety of values, where the distribution has a well-defined maximum value, $\Omega_{\max}$, which is typically close but not identical to the average $\langle\Omega\rangle$ [22]. For large systems, both $\Omega_{\max}$ and $\langle\Omega\rangle$ will equal $\omega_0 \approx 0.3868$ at $T = 0$ and approach $\frac{6}{13} \sim 0.46$ as $T \to \infty$. The first order nature of the transitions between the different commensurate phases can be verified by looking at the distribution of Ω near the transitions, which exhibits two well separated peaks, with one overtaking the other as the transition temperature is crossed [19]. This suggests that $\Omega_{\max}(T)$ is a reliable indicator of these transitions.

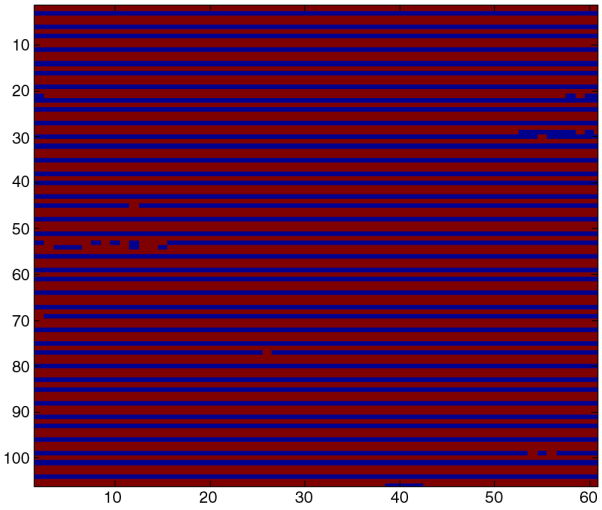

FIG. 4 (color online). Finite temperature configuration averaged over time exhibiting $\frac{3}{8}$ periodicity. The row structure is evident, with colors as in Figure 1. Here $L = 150$, $J_x = J_y$, and $T = 0.304$. Note that type B rows appear only in singles, while there can be two successive type A rows.

In Fig. 5, we show curves of $\Omega_{\max}$ and the specific heat C_V vs T, for a 150×150 system. At low temperature, the system is in its ground state, and $\Omega_{\max} = \omega_0$ (to within $\frac{1}{L}$). As temperature is increased, $\Omega_{\max}$ undergoes three jump discontinuities before becoming fully continuous as the rows are no longer homogeneous. While the stepwise behavior of $\Omega_{\max}$ is a clear indication of the existence of the commensurate phases and the first order nature of the transitions between them, its value at the plateaus does not give the exact periodicities due to limited resolution and the existence of defects, and these then must be inferred by looking at the configurations themselves, as in Fig. 4. The first order transitions are accompanied by small bumps in the specific heat at the same temperatures. In Fig. 5, we identify phases with periods of 8 and 13 rows with the lower and middle plateaus, respectively. In our examinations of systems of sizes up to $L = 300$, we have identified phases with $\Omega = \frac{1}{3}, \frac{3}{8}, \frac{5}{13}, \frac{7}{18}$, and $\frac{8}{21}$, depending on system size and values of the coupling constants [23]. At these temperatures, we have verified numerically that the rows substantially maintain their pure A or B character. The broad peak in the specific heat at $T \sim 0.37$ attends the loss of purity in the rows.

These results may be understood by an effective coarse-grained description of this system, appropriate for low temperatures, when the system may be considered as composed of A and B type rows [24]. This description resembles the Frenkel-Kontorova model [16], and exhibits a competition between length scales. To see this, note that for the perfect tiling, the value of the frequency α_n for the nth row may be calculated from the tile markings: $\alpha_n = \lim_{L\to\infty} \frac{1}{L} \sum_{m=1}^{L} t_{mn}$. From this, using Eqs. (5) and (6), we can compute ϕ_n. Now, although defects enter the rows at

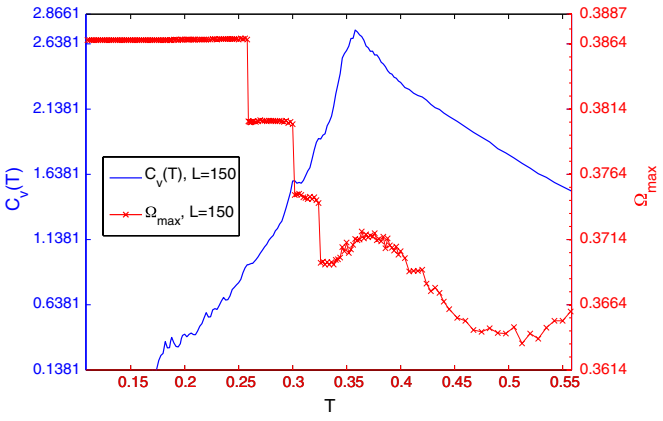

FIG. 5 (color online). $\Omega_{\max}$ and C_V as a function of temperature, for a 150×150 system with $J_x = J_y$.

finite T, we may still define two frequencies, using the markings of the top and bottom of a row. The "top frequency" is defined as $\alpha_n^T = \frac{1}{L}\sum_{m=1}^{L} t_{mn}$ while the "bottom frequency" is given by $\alpha_n^B = \frac{1}{L}\sum_{m=1}^{L} b_{mn}$. For a perfect tiling, $\alpha_n^B = \alpha_{n+1}^T$, and therefore, from Eq. (1), $\alpha_n^B/\alpha_n^T = q_n$, but this will typically not be the case for defected tilings. This notwithstanding, the ϕ_n at finite T may be inferred from α_n^T using Eq. (6) in the same manner as for the perfect tiling. These will be the variables used in our effective description.

To construct an effective free energy for this model we assume that the dominant contributions come from the entropy of the rows, and the energy due to mismatches between the rows, each of which is characterized by its frequencies α^T and α^B . We argue that the energy cost associated with an imperfect interface between rows n and $n+1$ goes as $LJ_y|\alpha_n^B - \alpha_{n+1}^T|$, where L is the length of the row. Clearly, this term is zero in the ground state, and numerical simulations bear out this functional form for low temperatures [19]. At this level of coarse graining, a row is characterized by its frequency α^T (or equivalently α^B), and its entropy should be a function of this frequency which is extensive in L, so that we shall write the entropy of the nth row as $L\tilde{s}(\alpha_n^T)$.

Taken together, we get that the free energy is given by $F/L = \sum_{n=1}^{L} J_y|q_n\alpha_n^T - \alpha_{n+1}^T| - T\tilde{s}(\alpha_n^T)$. It is convenient to express this in terms of the variables ϕ_n discussed above. The free energy is then of the form

$$\frac{F}{L} = \sum_m J_y g(\phi_m, \phi_{m+1}) - Ts(\phi_m), \tag{7}$$

where $g(\phi_m, \phi_{m+1})$ is a function that favors $\phi_{m+1} = \phi_m + \omega_0$, which holds identically in the ground state. The entropy $s(\phi_n)$ depends only on the fractional part $\{\phi_n\}$, and thus it is a periodic function with period one. It is the competition between these two length scales which gives the novel behavior observed. Although it is tempting to expand $g(\phi_n, \phi_{n+1})$ to first order as $g(\phi_n, \phi_{n+1}) \propto |\phi_{n+1} - \phi_n - \omega_0|$, we note that such an expression fails when both $\{\phi_n\}$ and $\{\phi_{n+1}\}$ are larger than $1 - \omega_0$, since this would imply two adjacent B rows, which carries a disproportionately large energy cost.

The equilibrium configuration of the ϕ_n can be obtained by minimizing F. As in the FK model, the first term favors an incommensurate phase with a winding number ω_0 while the entropy favors a commensurate configuration. The temperature T plays the role of the strength of the periodic potential, so that commensurate phases are expected at high temperature, while incommensurate phases are expected at low temperatures. The commensurate phases that are expected are those with a winding number close to ω_0 such as $1/3$, $3/8$, $5/13$, etc. We have observed some of these phases in our numerical study, as seen in Fig. 5, where their presence is indicated by the plateau values of $\Omega_{\max}$. At still higher temperatures the segregation into type A and B rows breaks down, resulting in a disordered phase. It is interesting to speculate about the low T behavior of this system. It might be that only at $T = 0$ an incommensurate phase appears, but it could be that such a phase, possibly with power-law correlations, is stable at finite T. These issues will be addressed in future research.

We would like to thank P. Chaikin, J. Kurchan, T. Lubensky, F. Sausset, and G. Wolff for fruitful discussions. D. L. gratefully acknowledges support from Israel Science Foundation Grant No. 1574/08 and US-Israel Binational Science Foundation Grant No. 2008483.

[1] As distinct, for example, from the Heisenberg or x-y models, which employ continuous spins.
[2] B. Grünbaum and G. Shephard, *Tilings and Patterns* (W. H. Freeman and Company, New York, 1987).
[3] Wang tilings employ square tiles, and as such, may be used to model systems on a square lattice.
[4] C. Radin, Ann. Math. **139**, 661 (1994).
[5] G. Wolff and D. Levine, arXiv:1302.5077.
[6] H. Koch and C. Radin, J. Stat. Phys. **138**, 465 (2010).
[7] L. Leuzzi and G. Parisi, J. Phys. A **33**, 4215 (2000).
[8] Z. Rotman and E. Eisenberg, Phys. Rev. E **83**, 011123 (2011).
[9] D. Aristoff and C. Radin, J. Phys. A **44**, 255001 (2011).
[10] J. Miekisz, J. Stat. Phys. **58**, 1137 (1990).
[11] T. W. Byington and J. E. S. Socolar, Phys. Rev. Lett. **108**, 045701 (2012).
[12] S.-i. Sasa, Phys. Rev. Lett. **109**, 165702 (2012).
[13] S.-i. Sasa, J. Phys. A **45**, 035002 (2012).
[14] K. Culik, II, Discrete Math. **160**, 245 (1996).
[15] J. Kari, Discrete Math. **160**, 259 (1996).
[16] P. M. Chaikin and T. C. Lubensky, *Principles of Condensed Matter Physics* (Cambridge University Press, Cambridge, England, 2000).
[17] M. Baake, F. Gähler, and U. Grimm, Symmetry **4**, 581 (2012).
[18] J. Eigen, S. Navarro, and V. Prasad, in *Proceedings of the MSRI Conference on Recent Progress in Dynamics* (MSRI Publications, Berkeley, CA, 2007), Vol. 54, p. 207.
[19] N. Nikola, D. Hexner, and D. Levine (to be published).
[20] J. Allouche and J. Shallit, *Automatic Sequences: Theory, Applications, Generalizations* (Cambridge University Press, Cambridge, England, 2003).
[21] J. Kurchan and D. Levine, J. Phys. A **44**, 035001 (2011).
[22] The distinction between $\Omega_{\max}$ and $\langle\Omega\rangle$ will vanish in the thermodynamic limit.
[23] We note that while this series of phase transitions bears a resemblance to the transitions with a growing period found in hierarchical tilings derived from a substitution rule [10,11], the two models are, in fact, fundamentally different; in the KC system there are no periodic motifs in the ground state, no sublattices which freeze at their respective transitions, and each transition entails a system-wide reordering.
[24] Although this is easiest to justify when $J_x > J_y$, our numerical study indicates that it has a large range of validity even when $J_x = J_y$.